Interaction with 14-3-3 Adaptors Regulates the Sorting of hMex-3B RNA-binding Protein to Distinct Classes of RNA Granules

Julien Courchet, Karine Buchet-Poyau, Auriane Potemski, Aurélie Brès, Isabelle Jariel-Encontre, Marc Billaud

THE JOURNAL OF BIOLOGICAL CHEMISTRY VOL. 283, NO. 46, pp. 32131–32142, November 14, 2008

Interaction with 14-3-3 Adaptors Regulates the Sorting of hMex-3B RNA-binding Protein to Distinct Classes of RNA Granules*[S]

Received for publication, April 16, 2008, and in revised form, September 8, 2008 Published, JBC Papers in Press, September 8, 2008, DOI 10.1074/jbc.M802927200

Julien Courchet[‡1], Karine Buchet-Poyau[‡2], Auriane Potemski[‡], Aurélie Brès[‡], Isabelle Jariel-Encontre[§], and Marc Billaud[‡3]

From the [‡]CNRS UMR5201, Laboratoire de Génétique Moléculaire, Signalisation et Cancer, Lyon F-69008, France, Université de Lyon, Lyon F-69008, France, Université Lyon 1, Domaine Rockefeller, Lyon F-69008, France, and Centre Léon Bérard, Lyon F-69008, France and [§]Institut de Génétique Moléculaire de Montpellier, CNRS, 1919 Route de Mende, Montpellier F-34293, France

Stress granules (SG) and processing bodies (PBs) are cytoplasmic ribonucleoprotein particles whose assembly is induced by different stimuli. SG are the site of storage of untranslated transcripts formed in response to environmental stress, whereas PBs are involved in mRNA turnover. We recently characterized a novel family of four human proteins related to the *Caenorhabditis elegans* Mex-3, a RNA binding protein involved in the establishment of the anterior-posterior embryonic asymmetry and in the maintenance of germline pluripotency. We now report that the adaptor proteins 14-3-3 bind to hMex-3B but not to the three other hMex-3 family members. Serine 462, when phosphorylated, is the major 14-3-3 docking site on hMex-3B, and manipulation of this interaction reveals that 14-3-3 both stabilizes hMex-3B and modulates its ability to bind RNA. Furthermore, the complex formed between hMex-3B and Argonaute proteins is excluded from PBs when the interaction with 14-3-3 is disrupted, whereas the recruitment to SG is not affected. Thus, 14-3-3 exerts combined effects on hMex-3B and acts as a major regulator of the sorting between distinct classes of RNA granules.

The regulation of mRNA translation and degradation plays a central role in the control of eukaryotic gene expression. It is increasingly evident that these posttranscriptional processes require the compartmentalization of ribonucleoprotein complexes (mRNPs)[4] in various cytoplasmic microdomains. Processing bodies (PBs) are one class of these RNA granules that are the sites of mRNA degradation and of storage of nontranslated transcripts (1–4). PBs concentrate factors involved in the 5′-3′ degradative pathway mRNA (1, 5–7), in nonsense-mediated mRNA decay (8), in AU-rich element-mediated mRNA decay, and also in RNA-mediated silencing (4). Stress granules (SG) constitute another class of RNA granules larger than PBs. SG assembly is induced in plant and mammalian cells by various environmental stresses (3, 9), such as heat, UV irradiation, and oxidative conditions. These structures are highly dynamic, and upon disappearance of stress conditions, they disassemble rapidly. SG aggregate stalled translation initiation complexes, including untranslated mRNA loaded on the 40 S ribosomal subunit, a subset of translation initiation factors, helicases, exonucleases, and several types of RNA-binding proteins (3). A large body of work has demonstrated that SG function as a triage center, redirecting mRNA fated to be degraded to PBs or allowing their transport to the cytoplasm where translation is reinitiated on polysomes (10, 11). Furthermore, evidence has been obtained that relatively fixed SG interact with more motile PBs via a set of shared proteins, a docking process that is believed to favor the exchange of mRNAs between these two compartments (11, 12). However, information on the mechanisms that finely tune the sorting of mRNPs between SG and PBs is still lacking.

We and others have recently identified a family of four human genes homologous to the *Caenorhabditis elegans Mex-3* that codes a RNA-binding protein which contains two tandemly repeated heterogeneous nuclear ribonucleoprotein K homology (KH) domains (13, 14). In the nematode, MEX-3 acts as a translational regulator that specifies posterior blastomere identity in the early embryo and contributes to the maintenance of germline totipotency (15–18). Human Mex-3 proteins (hMex-3A to -3D) are related RNA binding phosphoproteins that shuttle between the nucleus and the cytoplasm and display differential localization to PBs (14). We previously reported that hMex-3A and hMex-3B colocalize with the hDcp1a decapping factor in PBs, whereas hMex-3C is diffusely distributed in the cytoplasm. Furthermore, hMex-3 proteins display distinct modes of association with a subset of Argonautes proteins (Ago-1 and Ago-2), which are components of the RNA-induced silencing complex, the large key effector ribonucleoprotein complex of microRNA and of RNA interference pathways.

14-3-3s constitute a family of evolutionarily conserved, small acidic proteins that bind phosphorylated serine or threonine

* The costs of publication of this article were defrayed in part by the payment of page charges. This article must therefore be hereby marked "*advertisement*" in accordance with 18 U.S.C. Section 1734 solely to indicate this fact.

[S] The on-line version of this article (available at http://www.jbc.org) contains supplemental "Materials and Methods," Figs. 1–3, and Table 1.

[1] Recipient of a grant from the CNRS and from the Association pour la Recherche sur le Cancer.

[2] Recipient of a grant from the Centre Regional de Lutte contre le Cancer Léon Berard.

[3] To whom correspondence should be addressed. E-mail: billaud@univ-lyon1.fr.

[4] The abbreviations used are: mRNP, ribonucleoprotein complex; SG, stress granules; PB, processing bodies; KH, K homology; TAP, tandem affinity purification; YFP, yellow fluorescent protein; TTP, tristetraprolin protein; YN, amino-terminal fragment; YC, carboxyl-terminal fragment; hMex, human Mex; GFP, green fluorescent protein; HA, hemagglutinin; PBS, phosphate-buffered saline; AMCA, aminomethylcoumarin acetate.

residues (19). Seven mammalian isoforms of 14-3-3 proteins (β, γ, ϵ, ζ, η, τ, and σ) have been identified that can form homo- or heterodimers and show little isoform specific substrate specificity except for the 14-3-3σ isoform (20). 14-3-3 binding regulates client protein localization or function, and 14-3-3s are involved in cell functions such as cell cycle, apoptosis, and cell metabolism (19). Here we report that 14-3-3 proteins associate specifically with hMex-3B but not with the three other hMex-3 proteins. Interaction with 14-3-3 depends on the phosphorylation of hMex-3B on serine 462, and this binding stabilizes hMex-3B protein and modulates its ability to bind RNA. Moreover, formation of this complex is a key step that regulates the sorting of both hMex-3B and associated-Ago proteins between PBs and SG, thus indicating that 14-3-3 is a modulator of the dynamic exchange of mRNPs that links PBs and SG.

MATERIALS AND METHODS

Constructs and Mutagenesis—Coding sequences for hMex-3A, hMex-3B, hMex-3C, and p62-sequestosome were cloned in pCMV-Tag3B vector (Stratagene) as described previously (14). GFP-hDcp1a (a gift from B. Seraphin), pIRESneo-FLAG/HA Ago1 (a gift from T. Tuschl), pEYFP-Difopein (a gift from H. Fu), and pCS2+-HA-14-3-3eta (a gift from K. Blackwell) constructs were also used. Cloning of hMex-3D, pCMV-TAP, and pCMV-hMex-3B mutants and truncated forms is described under supplemental "Materials and Methods."

Antibodies—Mouse monoclonal anti-myc (9E10), anti-GFP (Roche Applied Science), anti-HA 11 (Covance), anti-actin (ICN), and anti-human PABP1 (10E10) (Sigma) antibodies were used in Western blots at 1:5,000, 1:1,000, 1:1,000, 1:25,000, and 1:2,000 dilutions, respectively. Anti-Myc, anti-GFP, and anti-HA antibodies were also used in immunofluorescence at 1:300 dilution. Rabbit polyclonal anti-M3Bß antibody was used for immunofluorescence and Western blots at 1:150 and 1:1000 dilutions, respectively. Mouse monoclonal anti-14-3-3β (H-8) antibody (Santa Cruz Biotechnology) and anti-Phospho(Ser) 14-3-3 binding motif (4E2) antibody (Cell Signaling) were used in Western blots at 1:1000 dilution. Goat polyclonal anti-TIA-1 (C-20), rabbit polyclonal anti-eIF4G, and mouse monoclonal anti-P70-S6 kinase, which cross-reacts with the PBs component HEDLS (human enhancer of decapping large subunit) (21) (Santa Cruz Biotechnology), were used in immunofluorescence at 1:100 dilution.

Cell Culture and Transfections—MCF7, HEK293, and BOSC cells were grown in Dulbecco's modified Eagle's medium with 4.5 g/liter glucose containing 10% fetal bovine serum, 100 units/ml penicillin, and 0.1 mg/ml streptomycin. HeLa cells were grown in Dulbecco's modified Eagle's medium with 1 g/liter glucose supplemented with 10% fetal bovine serum, 100 units/ml penicillin, and 0.1 mg/ml streptomycin. Cells were cultured at 37 °C in 5% CO_2. Cells were plated 24 h before transfection, and then plasmids were transfected into cells using ExGen 500 (Upstate Biotechnologies) or Lipofectin (Invitrogen) as a transfection reagent according to the manufacturer's instructions. When indicated, the phosphatase inhibitor calyculin A (Calbiochem) was used at 50 nM for 30 min.

Tandem Affinity Purification and Mass Spectrometry—TAP-tagged hMex-3B protein was expressed in HEK293 cells. Cells were harvested and lysed 48 h after transfection. TAP purification was performed as described previously (22) (see a detailed protocol under supplemental "Materials and Methods"). Tandem affinity purification (TAP) protein complexes were submitted to SDS-PAGE on a Tris-HCl gradient precast gel (Bio-Rad). Mass spectrometry analysis is described under supplemental "Materials and Methods".

Protein Analyses and Immunoprecipitation—Cells were lysed 48 h post-transfection, and Western blot analyses and immunoprecipitations were performed as described earlier (14, 23) (see supplemental "Materials and Methods"). Quantitative Western blot analyses were performed using Li-Cor Odissey (Li-Cor Biosciences) according to the manufacturer's instruction (see supplemental "Materials and Methods").

For immunoprecipitation, Myc-tagged proteins were immunoprecipitated from protein extracts (1 mg) with the anti-Myc antibody (5 μg) as described earlier, and Western blot analyses were performed as described on the immunocomplexes obtained.

To test for the phosphorylation of proteins, protein extracts prepared in lysis buffer without phosphatase inhibitors were treated for 1 h at 37 °C with 8 units of λ-phosphatase (Biolabs) per μg of protein. Protein extracts were treated with or without RNase A (0.2 mg/ml) before immunoprecipitation.

Immunofluorescence—BOSC, MCF7, or HeLa cells were plated on glass coverslips and were transiently transfected as described. After 48 h, cells were fixed for 20 min in 4% paraformaldehyde, permeabilized 5 min in 0.5% Triton X-100, and blocked 20 min in PBS containing 0.3% bovine serum albumin. Cells were then incubated overnight with primary antibody diluted in PBS, bovine serum albumin at 4 °C and were incubated 1 h with fluorescent-labeled secondary antibody at room temperature. Cells were mounted with DakoCytomation Fluorescent Mounting Medium (DakoCytomation) and were observed with a confocal microscope TSC SP2 (Leica) at the Centre Commun de Quantimetrie (Université Claude Bernard Lyon I). For BiFC, cells were incubated for 4 h at 30 °C before immunofluorescence as described above to increase YFP maturation and yellow fluorescence.

For characterization and quantification of hMex-3B containing granules, cells were transfected and stained as described above, and protein localization was observed by confocal microscopy. The size of hMex-3B-containing granules and colocalization with hDcp1 and TIA1 was evaluated for each transfected cell analyzed.

Protein Half-life Determination—HeLa cells were transfected as described in 100-mm dishes, then were trypsinized 24 h after transfection and plated in 60-mm wells. Cells were treated with 100 μg/ml cycloheximide (Sigma) for the indicated times before lysis. Protein samples were analyzed by Western blotting. Signal intensity was quantified using a FluorS Multimager and QuantityOne (Bio-Rad).

RESULTS

14-3-3 Adaptor Proteins Interact Specifically with hMex-3B—To identify proteins interacting with hMex-3B, a TAP analysis was undertaken (22, 24). The TAP tag was fused to the amino-terminal region of hMex-3B, and we verified that the tag did not

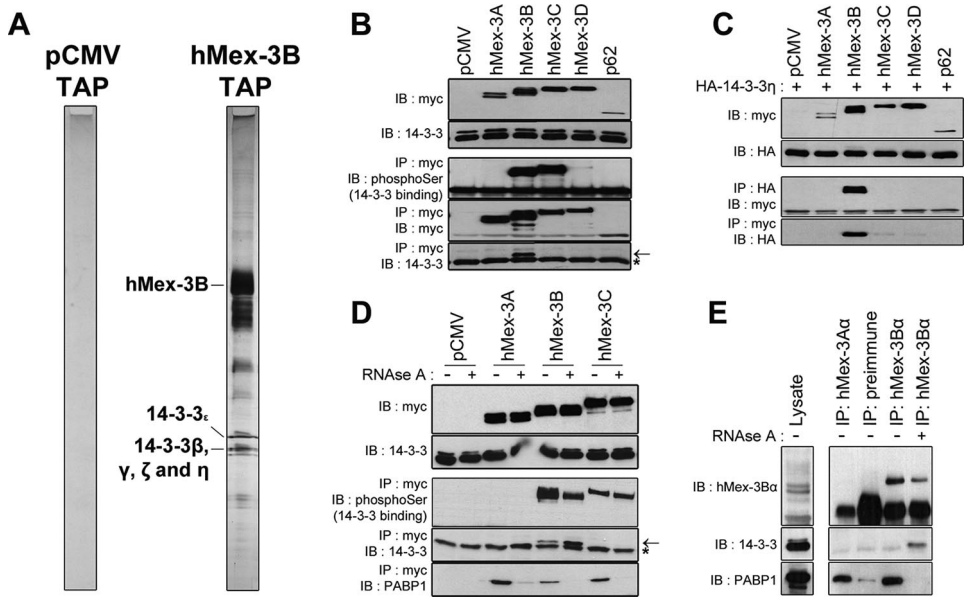

FIGURE 1. **hMex-3B interacts specifically with 14-3-3 proteins.** *A*, TAP analysis of hMex-3B-associated proteins. TAP-tagged hMex-3B was expressed in HEK293 cells, and protein complexes were purified by TAP. Samples were submitted to SDS page on an 8–16% gradient gel and silver-stained. Proteins were identified by MS/MS analyses. *B–D*, BOSC cells were transiently transfected with the plasmids coding Myc-tagged hMex-3 proteins together with HA-tagged 14-3-3η when indicated. Western blot analyses were performed on samples before or after immunoprecipitation (*IP*) with the indicated antibodies. All samples were loaded on an 11% SDS-polyacrylamide gel, and immunoblot (*IB*) analyses were performed with the indicated antibodies. When indicated (+), cell lysates were treated with RNase A (0.2 mg/ml) for 30 min at room temperature. *B–C*, co-immunoprecipitation between hMex-3B and endogenous (*B*) or exogenously expressed 14-3-3 proteins (*C*). RNase treatment of the lysate increases hMex-3B-14-3-3 interaction (*D*). *E*, co-immunoprecipitation between endogenously expressed hMex-3B and 14-3-3 proteins. hMex-3B immunoprecipitation from 15 mg of non-transfected BOSC cells lysate was performed using anti-hMex-3Bα antibody, whereas anti-hMex-3Aα and rabbit preimmune serum were used as precipitation negative control. RNase A treatment (0.2 mg/ml, 30 min) was performed when indicated. Samples were submitted to SDS-page on an 11% acrylamide gel, and IB was performed with the indicated antibodies. *Arrow*, 14-3-3 proteins. *, IgG light chain.

alter hMex-3B subcellular localization (data not shown). Upon transient transfection in HEK293 cells, TAP-tagged hMex-3B affinity-purified complexes were resolved on a 8–16% gradient SDS-PAGE and silver-stained. Whereas no proteins were purified using an empty pCMV-TAP vector as a negative control, two independent TAP analyses with TAP-tagged hMex-3B revealed two prominent bands between 30 and 33 kDa that were identified as five different isoforms of 14-3-3 proteins by mass spectrometry analysis (Fig. 1*A* and supplemental Table 1).

To verify the interaction between hMex-3B and 14-3-3 proteins, Myc-tagged hMex-3 proteins were transiently expressed in BOSC cells. Cells were lysed in mild conditions that preserve protein-protein interactions followed by immunoprecipitation with an anti-Myc antibody, and immunoblots were probed using an antibody that recognizes the seven known mammalian isoforms of 14-3-3. Under these conditions, endogenous 14-3-3 proteins were specifically co-immunoprecipitated with hMex-3B protein (Fig. 1*B*). Interestingly, this interaction was specific to hMex-3B as 14-3-3 proteins did not co-immunoprecipitate with either hMex-3A, -3C, or -3D. To further confirm the specificity of this interaction, BOSC cells were transfected with plasmids encoding hMex-3 proteins and HA-tagged 14-3-3η (one of the 14-3-3 isoforms identified by TAP analysis). Proteins were immunoprecipitated using anti-Myc or anti-HA antibodies, and immunoblotting analyses confirmed the specific association of hMex-3B and 14-3-3η (Fig. 1*C*). A much weaker interaction was also detectable between 14-3-3η and hMex-3C and -3D. Although hMex-3A expression is always lower than expression of other hMex-3 proteins, coprecipitation of 14-3-3η with hMex-3A was never observed ever with a stronger expression. Similarly, 14-3-3 proteins coimmunoprecipitated with hMex-3B in HeLa cells (supplemental Fig. 1).

We next sought to determine whether hMex-3B/14-3-3 interaction was mediated by an mRNA bridge. hMex-3 proteins were expressed in BOSC cells, and the protein lysate was treated or not with RNase before immunoprecipitation. 14-3-3 coprecipitation was not abolished by RNase treatment (Fig. 1*D*); on the contrary, we observed that 14-3-3 interaction with hMex-3B was enhanced after RNase treatment. This result, thus, suggests that hMex-3B and 14-3-3s are part of the same protein complex and that hMex-3B/14-3-3 interaction increases when hMex-3B is not bound to mRNA.

To further extend the physiological significance of these data, endogenously expressed hMex-3B protein was immunoprecipitated from BOSC cells with or without RNase treatment of the lysate. 14-3-3s did not coimmunoprecipitate either with a control preimmune rabbit serum or with an antibody directed against hMex-3A (Fig. 1*E*). A complex between hMex-3B and 14-3-3 can be observed only after RNase treatment of the lysate. Thus, this result confirms that endogenously expressed hMex-3B and 14-3-3s can form a complex under specific conditions.

Interaction with 14-3-3 Requires Phosphorylation of hMex-3B on Ser-462—To determine which region of hMex-3B is necessary for 14-3-3 binding, we generated several truncated forms of hMex-3B consisting of the deletion of either the amino-terminal region containing the two KH domains involved in mRNA binding, the carboxyl-terminal domain containing the E3 ubiquitin-ligase RING domain, or the linker part (Fig. 2*A*). All corresponding proteins were expressed at similar levels in BOSC cells, except the hMex-3B 1–433 mutant protein, which was occasionally slightly less abundant (Fig. 2*B* and data not shown). Coprecipitation of 14-3-3 proteins to hMex-3B was still observed with the truncated forms that possess the carboxyl-terminal domain (hMex-3B Δ239–433 and 239–569) and even enhanced with the amino-terminal-deleted form (hMex-3B 239–569). On the contrary, 14-3-3 proteins did not associate with the truncated forms in which the carboxyl-terminal fragment was deleted (hMex-3B 1–433, 1–239, and 239–

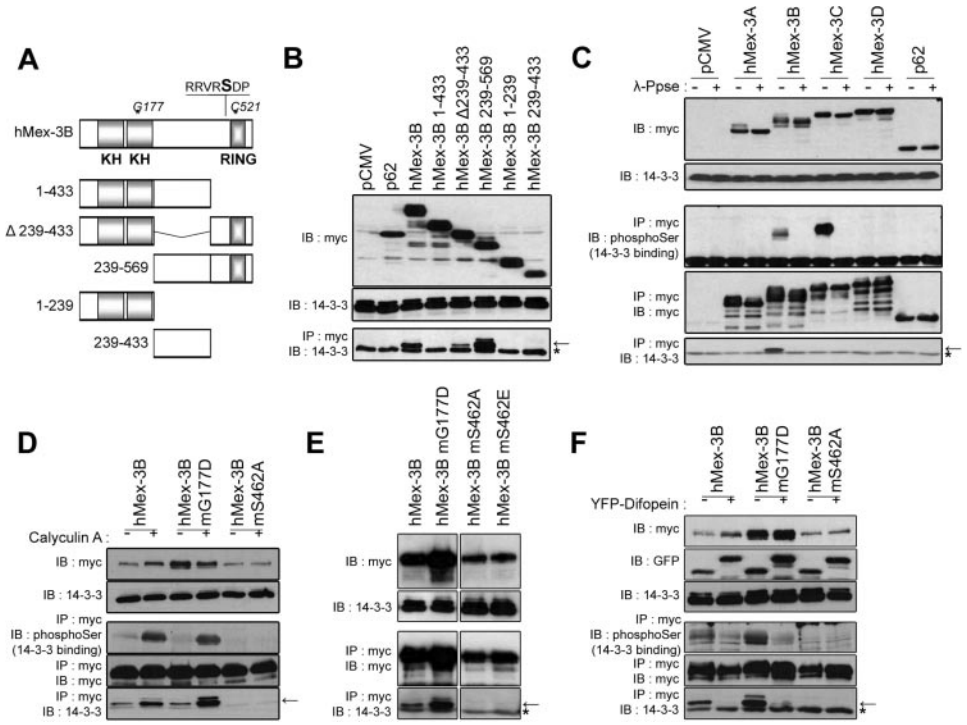

FIGURE 2. **hMex-3B/14-3-3 interaction requires phosphorylation of hMex-3B at Ser-462.** BOSC cells were transiently transfected with the indicated plasmids, and hMex-3 proteins were precipitated when indicated (*IP*) with anti-Myc antibody. All samples were loaded on an 11% SDS-polyacrylamide gel, and immunoblot (*IB*) analyses were performed after immunoprecipitation or directly on the lysate with the indicated antibodies. *Arrow*, 14-3-3 proteins. *, IgG light chain. *A* and *B*, mapping of 14-3-3 docking site on hMex-3B. *A*, hMex-3B protein is schematized with its functional domains. The truncated mutants used in this study are described. The sequence surrounding Ser-462 (*bold*) forms a 14-3-3 mode II binding sequence. *, position of residues Gly-177 and Cys-521, whose mutation abolish binding to mRNA or the RING structure, respectively. *B*, full-length hMex-3B and the truncated forms described above were expressed in BOSC cells. Western blot analyses were performed after anti-Myc immunoprecipitation or directly from the lysate. *C*, phospho-dependent interaction between hMex-3B and 14-3-3. Myc-tagged hMex-3 proteins were expressed in BOSC cells. When indicated (+), cell lysates were treated with λ phosphatase (*λ-Ppse*) for 30 min at 37 °C before immunoprecipitation. Western blot analysis was performed with the indicated antibodies. *D* and *E*, phosphorylation of hMex-3B Ser-462 is necessary for 14-3-3 binding. BOSC cells were transfected with vectors coding Myc-tagged wild-type hMex-3B or mutant proteins. 48 h post-transfection, cells were treated with DMSO (−) or calyculin A (+) (50 nM, 30 min) before lysis, and immunoprecipitation were carried out. Western blot analysis was performed with the indicated antibodies. *F*, hMex-3B binds to 14-3-3 proteins within their amphipathic groove. Myc immunoprecipitation was performed from BOSC cell lysates coexpressing either the wild-type or mutant hMex-3B protein together with the 14-3-3 inhibitor YFP-Difopein when indicated (+). peGFP vector was used as a negative control in comparison with YFP-Difopein (−). Western blot analysis was performed with the indicated antibodies.

433). These data indicate that hMex-3B carboxyl-terminal region is necessary for hMex-3B/14-3-3 interaction.

14-3-3s constitute a family of related-proteins that bind to a phosphorylated serine/threonine residue embedded in a specific peptide sequence (19). However, association of 14-3-3s with certain "client" proteins can also occur in a phosphorylation-independent manner (25). To examine whether hMex-3B/14-3-3 interaction is phosphorylation-dependent, hMex-3B proteins were expressed in BOSC cells, and protein extracts were dephosphorylated or not by λ-phosphatase treatment before immunoprecipitation with the anti-Myc antibody. Immunoblot analysis showed that 14-3-3 proteins coimmunoprecipitated specifically with hMex-3B in the absence of phosphatase treatment, whereas dephosphorylation of the lysate disrupted 14-3-3 interaction without changing reproducibly hMex-3B expression (Fig. 2*C*).

Sequence analysis revealed that the sequence surrounding Ser-462 (RRVRpS462DP) of hMex-3B conforms to a putative 14-3-3 mode-II binding motif (26). This serine was replaced by an alanine by site-directed mutagenesis to generate hMex-3B mS462A. BOSC cells were transfected with either the Myc-tagged hMex-3B, the S462A mutant, or with an additional mutant that we previously reported (14) that disrupts the second KH-domain (G177D) and abolishes mRNA binding both *in vitro* and *in vivo*. The cell-permeable phosphatase inhibitor calyculin A was added to the culture medium 30 min before lysis to reinforce hMex-3B phosphorylation, then hMex-3B proteins were immunoprecipitated with an anti-Myc antibody. The hMex-3B S462A mutant was reproducibly expressed at a lower level than the wild type, whereas hMex-3B G177D protein was more abundant (see below for a discussion of this point; Fig. 2*D*). 14-3-3 proteins co-immunoprecipitated with the wild-type hMex-3B and the KH-domain mutant, the coprecipitation being enhanced by calyculin A treatment. In contrast, 14-3-3 proteins failed to associate with hMex-3B S462A even with calyculin A treatment. Similarly, 14-3-3 proteins did not coimmunoprecipitate with a mutant form of hMex-3B where Ser-462 has been replaced by a phosphomimetic residue such as glutamic acid (hMex-3B mS462E, Fig. 2*E*), as has been described for other proteins (27, 28). We next employed a mouse monoclonal antibody that recognizes phosphoserine residues within a 14-3-3 binding consensus sequence (anti-phosphoserine 14-3-3 binding). A signal corresponding to hMex-3B was observed after immunoprecipitation with the wild-type and the KH (G177D) mutant, and this signal was increased upon phosphatase inhibition with calyculin A (Fig. 2*D*). This phosphoserine signal was lost when hMex-3B serine 462 was mutated to alanine even when cells were treated with calyculin A. In addition, a phosphoserine (14-3-3 binding) signal could be observed after hMex-3C and weakly after hMex-3D immunoprecipitation but not with hMex-3A (see Fig. 1*B*). The existence of a phosphoserine/threonine epitope on hMex-3C and hMex-3D is consistent with their weak binding to 14-3-3. Taken together, these results indicate that Ser-462 of hMex-3B is phosphorylated and is the major 14-3-3 docking site.

To further extend this analysis, we used the YFP-tagged Difopein, a competitive inhibitor of 14-3-3 (29). Difopein is composed of a tandemly repeated peptide sequence that binds 14-3-3 within

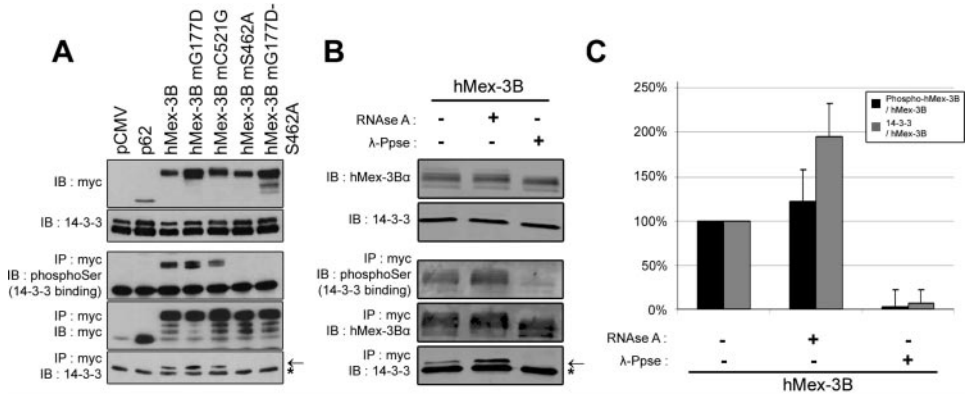

FIGURE 3. **hMex-3B/14-3-3 interaction modulates the binding to mRNA.** All samples were loaded on a 11% SDS-polyacrylamide gel, and immunoblot analyses were performed after immunoprecipitation or directly on the lysate with the indicated antibodies. *Arrow*, 14-3-3 proteins. *, IgG light chain. *A*, differential binding of hMex-3B mutants to 14-3-3 proteins. Myc-tagged wild-type hMex-3B or mutant proteins were expressed in BOSC cells and precipitated using anti-Myc antibody. Samples were loaded on a 11% SDS-polyacrylamide gel, and immunoblot (*IB*) analyses were performed after immunoprecipitation (*IP*) or directly on the lysate with the indicated antibodies. *Arrow*, 14-3-3 proteins. *, IgG light chain. *B* and *C*, quantification of 14-3-3 coimmunoprecipitation. *B*, wild-type hMex-3B protein was expressed in BOSC cells and precipitated using anti-Myc antibody. λ-Phosphatase (λ-*Ppse*, 30 min, 37 °C) or RNase A (30 min, room temperature) treatment were performed before immunoprecipitation as indicated. Quantitative Western blot analysis was realized using Li-Cor Odissey using IRDye 700DX coupled anti-rabbit (hMex-3Bα) and IRDye 800 coupled anti mouse antibodies (14-3-3, *phosphoSer*). *C*, the signal was quantified using Odissey software. hMex-3B phosphorylation (*black*) and 14-3-3 coimmunoprecipitation (*gray*) were compared with the amount of precipitated total hMex-3B for normalization. Histograms represent the mean values for three independent experiments. *Error bars*, S.D.

its amphipathic groove in a phosphorylation-independent manner. BOSC cells were transfected with either YFP-Difopein expression vector or empty peGFP plasmids together with the wild-type or mutant hMex-3B expression vectors. As shown on Fig. 2*F*, Difopein inhibited 14-3-3 binding to both the wild-type and the hMex-3B G177D mutant. 14-3-3 binding inhibition correlated with a decrease of hMex-3B Ser-462 phospho-signal for the wild-type or the G177D mutant, as revealed by anti-phosphoserine (14-3-3 binding) antibody. Thus, these data indicate that 14-3-3s bind hMex-3B via their amphipathic groove, and this binding protects Ser-462 from dephosphorylation, similarly to what has been shown for the phosphatase CDC25C (30).

Binding Properties of hMex-3B to mRNA and 14-3-3—RNase treatment increases hMex-3B/14-3-3 interaction without any reproducible change of hMex-3B Ser-462 phosphorylation (Fig. 1*D*). This result suggests a mechanistic link between mRNA binding and 14-3-3 docking to hMex-3B. Consistent with these findings, we found that more 14-3-3 coprecipitated with a hMex-3B-truncated protein that lacks the KH domains (Fig. 2*B*) or with the hMex-3B KH-domain mutant unable to bind mRNA (Figs. 2, *E* and *F*, and 3*A*) compared with the wild-type hMex-3B, although we observed that the KH mutant was always more expressed than wild-type hMex-3B (this point is discussed below). A mutation in the RING domain (C521G) did not perturb the association with 14-3-3, thus confirming the specificity of the effect observed with the KH mutant (Fig. 3*A*). On the contrary, we observed a slight, non-reproducible decrease of Ser-462 phosphorylation and 14-3-3 coprecipitation with this hMex-3B mutant (Fig. 3*A* and data not shown). As expected, a double mutation (S462A and G177D) abolished the increased interaction with 14-3-3.

To accurately quantify the effects of either RNase A or λ-phosphatase treatments on hMex-3B/14-3-3s association, we exploited the infrared fluorescence imaging system (Odissey/Li-COR), which allows a wide quantitative linear range and high sensitivity of detection in Western blots. As shown in Fig. 3, *B* and *C*, using this measurement we found that RNase A treatment increased by 2-fold 14-3-3s binding on hMex-3B, whereas it did not significantly modify the level of phosphoserine in a 14-3-3 binding site. As expected, upon λ-phosphatase treatment, the fixation of 14-3-3s on hMex-3B was completely lost. Taken together, these results suggest that 14-3-3s binding weakens the hMex-3B interaction with mRNA.

14-3-3 Binding Stabilizes hMex-3B Protein—During the course of our experiments, we repeatedly noticed that the hMex-3B S462A protein was expressed at a lower level than the wild-type hMex-3B, whereas the KH mutant was expressed at higher level. Because 14-3-3 binding is known to stabilize certain client proteins (31–33), we further explored this question. HeLa cells were transfected with plasmids encoding wild-type or mutant hMex-3B proteins together with the 14-3-3 inhibitor Difopein. 24 h post-transfection, cells were treated with the translation inhibitor cycloheximide and collected between 1 and 24 h of inhibition time. As shown on Fig. 4, Western blot analysis revealed a decrease of hMex-3B protein levels with a longer time course of cycloheximide treatment. In the absence of YFP-Difopein, hMex-3B G177D was more stable than the wild-type hMex-3B, whereas hMex-3B S462A was more rapidly degraded (Fig. 4*A*). Quantification of the signals obtained in 5 independent experiments followed by regression analysis indicated respective half-lives of 5.6, 11.8, and 4.4 h for hMex-3B, hMex-3B G177D, and hMex-3B S462A (Fig. 4*B*). Moreover, whereas the half-life of hMex-3B mS462A was practically unaffected when Difopein was expressed, those of the wild-type and G177D mutant hMex-3B proteins exhibited a marked decrease of stability to match that of hMex-3B mS462A (Fig. 4*C*). Quantitative analysis indicated a half-life of either 3.6, 4.4, and 3.6 h for wild-type, mG177D, and mS462A hMex-3B, respectively (Fig. 4*D*). Collectively, these results provide evidence that 14-3-3 binding stabilizes hMex-3B protein.

14-3-3 Regulates hMex-3B Differential Localization to P-Bodies and Stress Granules—It is well documented that the binding of 14-3-3s regulates the subcellular distribution of certain client proteins (19, 34). We previously reported that hMex-3B protein forms cytosolic spots that colocalize with the P-body marker hDcp1 (14), whereas the KH mutant distribution is homogenous in the cytoplasm. To investigate whether 14-3-3 binding to hMex-3B modifies its subcellular localization, hMex-3B and the S462A mutants were expressed in HeLa cells, and a series of confocal microscopic analyses using various markers of P-bodies and SG was undertaken. As shown in

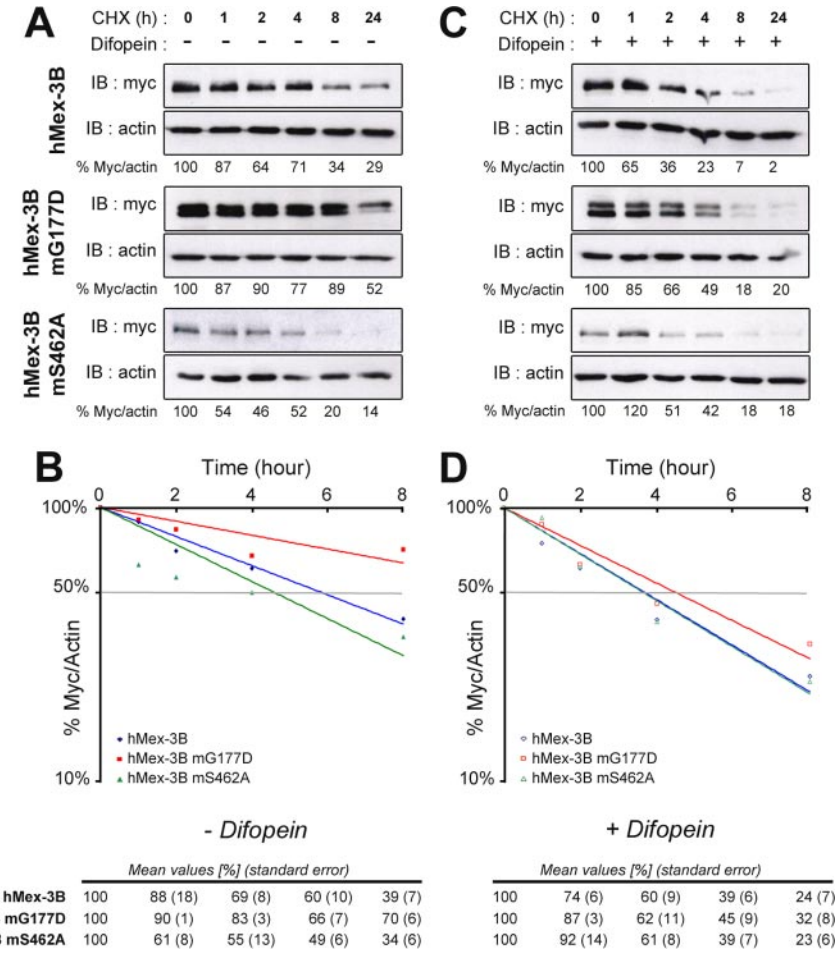

- Difopein

	Mean values [%] (standard error)				
hMex-3B	100	88 (18)	69 (8)	60 (10)	39 (7)
hMex-3B mG177D	100	90 (1)	83 (3)	66 (7)	70 (6)
hMex-3B mS462A	100	61 (8)	55 (13)	49 (6)	34 (6)

+ Difopein

	Mean values [%] (standard error)				
	100	74 (6)	60 (9)	39 (6)	24 (7)
	100	87 (3)	62 (11)	45 (9)	32 (8)
	100	92 (14)	61 (8)	39 (7)	23 (6)

FIGURE 4. **14-3-3 binding regulates hMex-3B protein stability.** HeLa cells were co-transfected with vectors expressing Myc-tagged wild-type hMex-3B or mutant proteins together with either eGFP (−) or YFP-Difopein (+). 24 h after transfection, cells were trypsinized and plated in 6-well plates. The translation inhibitor cycloheximide (*CHX*, 100 μg/ml) was added to the culture medium 24 h later for the indicated time. *A* and *C*, hMex-3B protein decay in the absence (*A*) or presence (*C*) of YFP-Difopein. Cells were lysed, and Western blot (*IB*) analysis was performed on an 11% SDS-polyacrylamide gel with anti-Myc and anti-actin antibodies. For each time point, Myc signal intensity was normalized to actin signal intensity. Signal intensity was 100% at the beginning of CHX treatment (*time 0*). Myc/actin ratio for the experiment shown on figure is indicated. *B* and *D*, quantification of normalized myc signal in cells expressing GFP (*B*) or YFP-Difopein (*D*). Five independent experiments were quantified. Each *dot* represents the mean quantification at the indicated time. The curves (plotted on a semilogarithmic graph) represent regression corresponding to the dots distribution. Mean values and S.E. corresponding to each time point are indicated *under the graphs*.

mS462A protein formed larger foci (52% of cells) than cells expressing wild-type hMex-3B (Fig. 5*B*), and this mutant protein mostly colocalized with TIA1 (57% of cells) but not with hDcp1 (Fig. 5, *C* and *D*), although in a few cells a weak signal corresponding to hDcp1 could occasionally overlap with hMex-3B positive granules. Similar results were also observed in BOSC and MCF7 cells (data not shown).

Overexpression of PBs components can generate abnormal PB structures that are not disrupted by emetine or cycloheximide treatment (3, 21). To confirm that hMex-3B containing granules are not aberrant granules due to hMex-3B overexpression, cells were treated with the translation inhibitor cycloheximide. As reported previously (14), hMex-3B localization was perturbed upon cycloheximide treatment, with most of the cells showing a diffuse relocalization of hMex-3B within the cytoplasm or showing small hMex-3B positive foci (Fig. 5*E*, *lower panel*). Together, these observations suggest that the binding of 14-3-3 modulates the differential localization of hMex-3B to P-Bodies and SG and that expression of hMex-3B promotes PB and SG fusion.

To determine in which cell compartment hMex-3B and 14-3-3 interact, HeLa cells were co-transfected with vectors expressing Myc-hMex-3B and HA-14-3-3η. In cells transfected with the empty vector pCMV, 14-3-3η was diffusely localized in the cytoplasm of the cells, and it neither colocalized with the PB marker hDcp1-GFP (Fig. 6*A*) nor with the SG marker TIA1 (Fig. 6*B*). In contrast, in cells expressing hMex-3B, 14-3-3η accumulated in cytoplasmic foci and colocalized both with hMex-3B and hDcp1 and with hMex-3B and TIA1, whereas expression of hMex-3B S462A did not induce any change in 14-3-3η cytoplasmic localization (data not shown). These results demonstrate that 14-3-3 and hMex-3B colocalize with PBs and SG.

We then turned to bimolecular fluorescence complementation o assess in which compartment the hMex-3B/14-3-3 complex accumulates *in vivo* (35). Two non-fluorescent fragments of the YFP protein, the amino-terminal fragment (YN) and the carboxyl-terminal fragment (YC), were fused to 14-3-3ϵ and hMex-3B, respectively. As expected, YN- and YC-tagged 14-3-3ϵ proteins were still able to form homodimer and coimmunoprecipitated with hMex-3B (supplemental Fig. 3). YC-14-

Fig. 5, *A* and *B*, hMex-3B is mainly localized in small cytoplasmic granules (53% of cells) which were similar to the morphology of P-bodies, as observed previously (14), but also in larger, SG-like foci (33% of cells). Confocal microscopic analyses of these larger foci revealed that h-Mex-3B colocalized both with the P-Bodies marker hDcp1 and with the SG marker TIA1 (3) (Fig. 5, *C* and *D*), whereas hDcp1 and TIA1 signal did not overlap when the empty vector pCMV was transfected into cells. To confirm these results, we repeated these experiments using an antibody that recognizes the translation initiation factor eIF4G, which shuttles to SG during stress (supplemental Fig. 2), and with an antibody that recognize the PB marker HEDLS (Fig. 5*E*, *upper panel*). These experiments confirmed that both PBs and SG markers colocalized in hMex-3B large granules, thus suggesting that expression of hMex-3B leads to the fusion of P-Bodies with SG as has been already described for other RNA-binding proteins (11). Strikingly, cells expressing hMex-3B

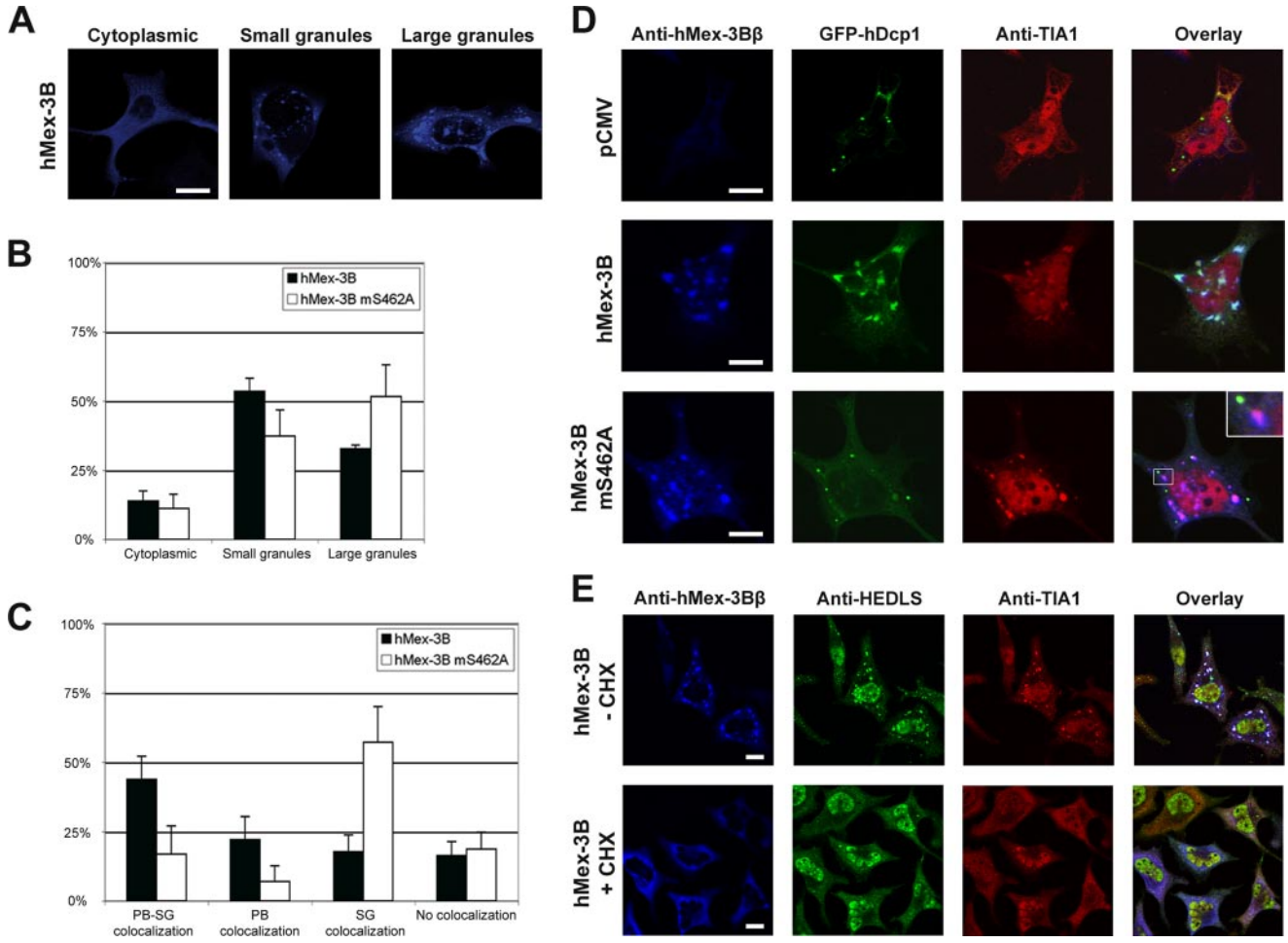

FIGURE 5. **14-3-3 binding regulates hMex-3B association to P-bodies and stress granules.** HeLa cells were co-transfected with vectors expressing Myc-tagged wild-type hMex-3B or mS462 mutant and GFP-hDcp1 as indicated. Proteins were stained with anti-Myc (*blue*), anti HEDLS (*green*), or anti-TIA1 (*red*) antibodies and revealed with AMCA-, Cy2-, and Cy5-conjugated secondary antibodies, respectively. Proteins colocalization was determined by confocal microscopy. *A* and *C*, different repartition of hMex-3B observed in HeLa cells. Confocal imaging of cells transfected with Myc-tagged hMex-3B coding vector showing the three localization patterns displayed by hMex-3B, diffuse in the cytoplasm (*left panel*) and forming small-size, PB-like (*center panel*) or large, SG-like granules (*right panel*). *Scale bar*, 10 μm. *B* and *C*, quantification of hMex-3B granule repartition. Localization of wild-type or mutant hMex-3B protein in transfected cells was quantified within different size of granules (*B*) and in colocalization with PB and SG markers (*C*). *Histograms* represent quantification of four independent experiments. *Error bars*, S.D. *D*, localization of hMex-3B within PBs and SG in HeLa cells. Wild-type or mutant hMex-3B proteins were expressed in cells together with GFP-hDcp1 protein. hMex-3B and endogenously expressed TIA1 protein localization was visualized by indirect immunofluorescence as indicated above. hDcp1 localization was visualized by direct GFP fluorescence (*green*). The *right panel* shows overlay of AMCA, GFP, and Cy5 signal. *E*, effect of cycloheximide (*CHX*) treatment on hMex-3B containing granules. hMex-3B-expressing HeLa cells were treated when indicated with CHX (10 μg/ml) for 1 h before fixation. hMex-3B protein localization (*blue*) was compared with the distribution of endogenous PB and SG markers HEDLS (*green*) and TIA-1 (*red*). The *right panel* shows an overlay of AMCA, Cy2, and Cy5 signal after confocal microscopy.

3-3ϵ and YN-hMex-3B coding plasmids were then transfected into HeLa cells, and protein localization was determined by indirect immunofluorescence. When expressed alone, neither YC-14-3-3ϵ nor YN-hMex-3B protein emitted a significant YFP fluorescence (Fig. 7), whereas coexpression of YC-14-3-3ϵ and YN-hMex-3B resulted in a detectable YFP fluorescence within cytoplasmic granules. Moreover, YC-14-3-3ϵ, which was diffused in the cytoplasm in the absence of YN-hMex-3B moiety, was actively recruited to cytoplasmic foci upon expression of YN-hMex-3B. Furthermore, expression of the YN-hMex-3B mutated on Ser-462 did not reconstitute YFP fluorescence with YC-14-3-3ϵ nor induce changes in 14-3-3ϵ localization, indicating that YFP fluorescence was specific to hMex-3B/14-3-3 complexes. Finally, colocalization experiments with TIA1 and HEDLS proteins showed that hMex-3B/14-3-3 complexes colocalized with PBs and SG markers (Fig. 7, *B* and *C*).

To directly examine if the binding of 14-3-3s is required for the sorting of hMex-3B between SG and PBs, we coexpressed Difopein and hMex-3B in MCF7 cells. As shown on Fig. 8*A*, Difopein did not alter hMex-3B and TIA1 colocalization, whereas it clearly reduced hMex-3B recruitment in HEDLS positive foci (Fig. 8*B*). Quantification of these results indicate that hMex-3B localization in PBs is 3-fold less abundant in MCF7 cells expressing Difopein *versus* control (Fig. 8*D*), whereas Difopein did not perturb hMex-3B localization in SG (Fig. 8*C*). Collectively, these data provide evidence that hMex-3B recruitment in PBs, but not in SG, depends on the fixation of 14-3-3s.

hMex-3B-Ago1 Complex Localization Is Regulated by 14-3-3 Binding to hMex-3B— hMex-3B interacts with the RNA-induced silencing complex component Ago1, and both proteins colocalize in cytoplasmic foci in HeLa cells (14). Because Ago1 is known to localize in PB and SG (36, 37), we investigated

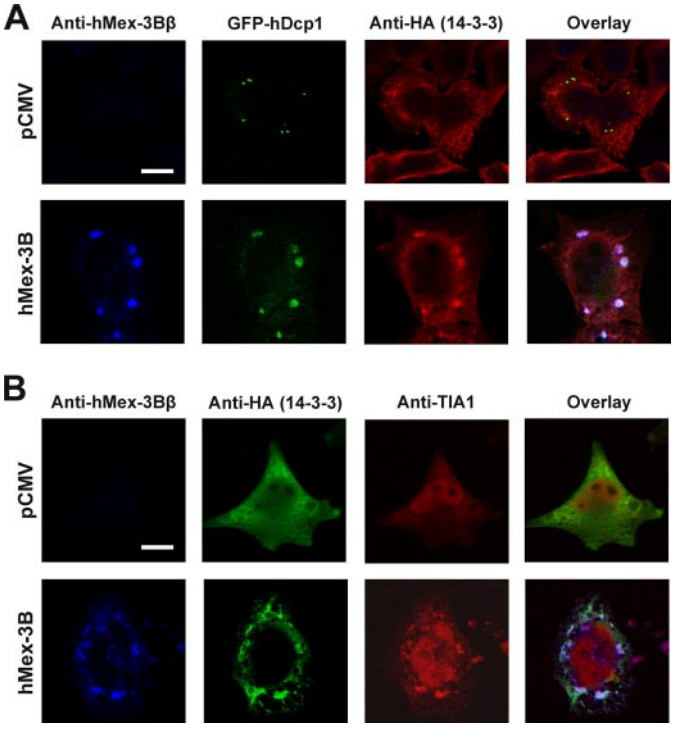

FIGURE 6. **14-3-3 proteins colocalize with hMex-3B in cytoplasmic foci.** *A* and *B*, colocalization of hMex-3B and 14-3-3 within PBs (*A*) or SG (*B*). Protein localization was determined by confocal microscopy. The *right panel* shows an overlay of AMCA, GFP/Cy2, and Cy5 signal. *Scale bar*, 10 μm. *A*, HA-tagged 14-3-3η protein was expressed in HeLa cells together with wild-type or mutant hMex-3B protein and GFP-hDcp1. Proteins were stained with anti-hM3Bβ (*blue*) or anti-HA (*red*) antibodies and revealed with AMCA- and Cy5-conjugated secondary antibodies, respectively. hDcp1 protein localization was visualized with GFP fluorescence (*green*). *B*, HA-14-3-3η and hMex-3B proteins were expressed in HeLa cells and visualized by indirect immunofluorescence using anti-hM3Bβ (*blue*) and anti-HA (*green*) antibodies, revealed with AMCA- and Cy2-conjuged antibodies, respectively. SG marker TIA1 was visualized by indirect immunofluorescence using anti-TIA1 (*red*) antibody revealed with Cy5-conjugated antibody.

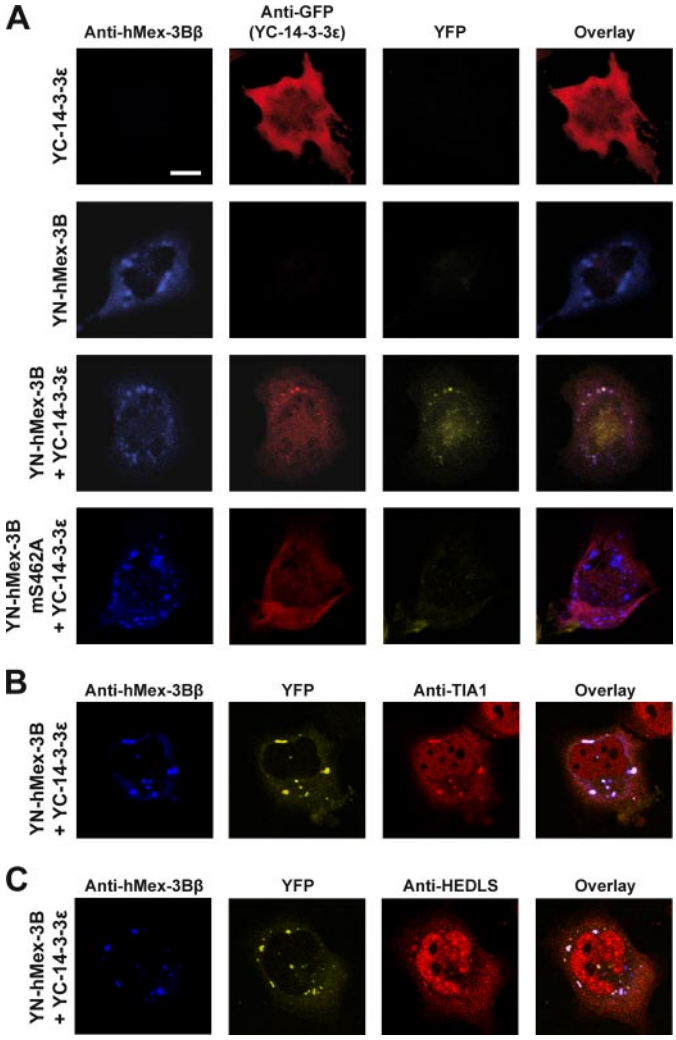

FIGURE 7. **hMex-3B and 14-3-3 interact in foci containing both PB and SG markers.** *A–C*, visualization of hMex-3B/14-3-3 complexes localization by bimolecular fluorescence complementation. YN-hMex-3B and YC-14-3-3ϵ coding plasmids were transfected in HeLa cells. hMex-3B/14-3-3 complexes were visualized by direct yellow (YFP) fluorescence. hMex-3B localization was determined by indirect immunofluorescence using anti-hM3Bβ (*blue*) antibody and revealed with AMCA-conjugated secondary antibody. hMex-3B/14-3-3 complex localization was compared with that of 14-3-3 (anti-GFP) (*A*), TIA1 (anti-TIA1) (*B*), or HEDLS (anti-HEDLS) (*C*) revealed with Cy5-conjugated secondary antibodies. Protein localization was determined by confocal microscopy. The *right panel* shows an overlay of AMCA, YFP, and Cy5 signal. *Scale bar*, 10 μm.

whether 14-3-3 binding to hMex-3B affects its interaction with Ago-1. HA-tagged Ago1 was expressed in BOSC cells together with wild-type or mutant Myc-hMex-3B, and proteins were immunoprecipitated with anti-Myc antibody with or without RNase treatment of the lysate. Western blot analysis revealed that, similarly to wild-type hMex-3B, hMex-3B mS462A associates with Ago1, and this interaction was lost after RNase treatment (Fig. 9*A*). As previously reported, a KH-mutant form of hMex-3B (hMex-3B mG177D) interacts with Ago1 in a RNA-independent manner (14).

The subcellular localization of Ago1 was then investigated by indirect immunofluorescence in HeLa cells. Plasmids encoding GFP-hDcp1 and HA-Ago1 were transfected in HeLa cells together with plasmids encoding wild-type or mS462A hMex-3B. Ago1 signal overlapped with hMex-3B signal, and both proteins colocalized perfectly with hDcp1 in PBs (Fig. 9*B*, quantified in Fig. 9*D*). In contrast, Ago1 protein colocalized with hMex-3B mS462A protein, but colocalization with hDcp1 was markedly decreased. We then examined the localization of hMex-3B and Ago1 within SG. As expected, Ago1 colocalized with both wild-type and S462A hMex-3B within TIA1-positive granules (Fig. 9, *C* and quantification in *D*). Taken together, these results show that hMex-3B interaction with the RNA-induced silencing complex component Ago1 is not influenced by 14-3-3 binding and that 14-3-3 binding to hMex-3B regulates not only the localization of hMex-3B to different RNA granules but also the localization of its cognate interactants.

DISCUSSION

In this report we showed that 14-3-3 proteins associate specifically with hMex-3B and not, or at most very weakly with hMex-3C and hMex-3D. This interaction with 14-3-3s, which is strictly dependent on the phosphorylation of hMex-3B on Ser-462, exerts several combined effects. First, the assembly of this complex stabilizes the hMex-3B protein; second, this fixation regulates hMex-3B RNA binding property; finally, 14-3-3s control the sorting of hMex-3B between PBs and SG.

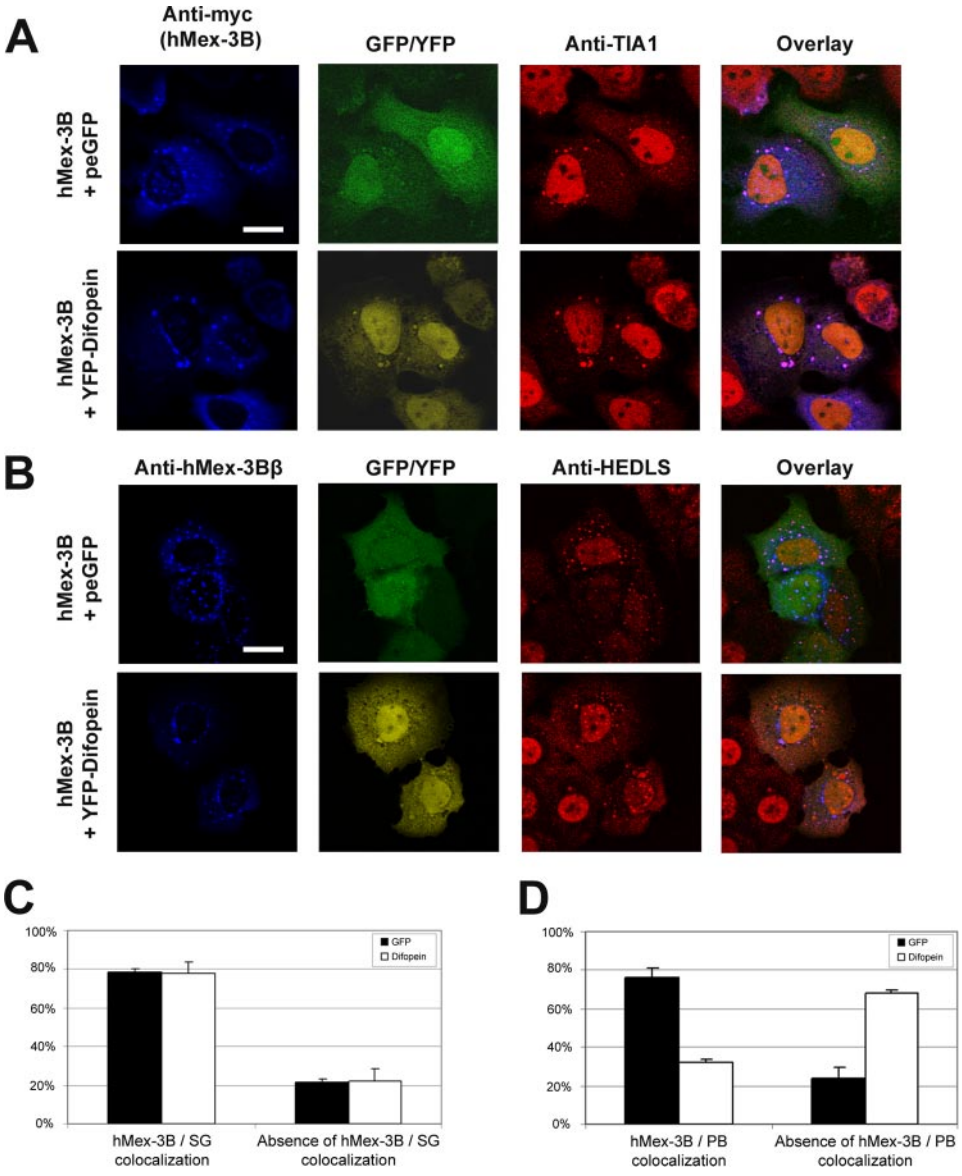

FIGURE 8. **Difopein disrupts hMex-3B localization in PBs.** *A* and *B*, confocal microscopy analyses of MCF7 cells co-transfected with vectors expressing Myc-tagged wild-type hMex-3B and either GFP or YFP-Difopein. hMex-3B localization was visualized by indirect immunofluorescence using anti-Myc or anti-hMex-3Bβ antibodies and revealed with AMCA-conjugated secondary antibodies. Colocalization with SG (*A*) and PBs (*B*) markers was performed using antibodies recognizing TIA1 and HEDLS (revealed by a Cy5-conjugated secondary antibody). GFP or YFP-Difopein signal was observed by direct fluorescence. Protein localization was determined by confocal microscopy. The *right panel* shows an overlay of AMCA, GFP/YFP, and Cy5 signal. *Scale bar*, 10 μm. *C* and *D*, quantification of hMex-3B association with PBs and SG. Cells showing colocalization of wild-type hMex-3B with PBs or SG markers were scored in three independent experiments. *Histograms* show the quantification of three independent experiments. *Error bar*, S.D.

14-3-3s Exert Multifarious Effects on hMex-3B—14-3-3s act as adaptor molecules which mediate several effects on their targets, including control of subcellular localization, regulation of enzyme activity, and stimulation of protein-protein interactions (19, 38). These molecules are also known to protect their target proteins from proteolysis and dephosphorylation. Given their versatile function, 14-3-3s are involved in a wide range of signaling pathways (34). 14-3-3s comprise seven distinct isoforms in mammals, and each one could bind hMex-3B. Although, we have not systematically addressed this question, our TAP analysis indicates that hMex-3B interacts with at least five different 14-3-3 isoforms.

14-3-3s form homo- or heterodimers, and each subunit recognizes phosphoserine or phosphothreonine in a sequence specific context. Three different phosphopeptides motifs that ligate 14-3-3s have been defined (26, 39, 40), and the sequence surrounding serine 462 of hMex-3B conforms to the type II. This sequence is also present in hMex-3C, and a different putative consensus sequence can be found in hMex-3D even though these proteins bind poorly to 14-3-3s, thus suggesting that additional protein surfaces are required to achieve a stable association with 14-3-3s. Accordingly, dimeric 14-3-3 frequently interacts with two separate phosphoserine or phosphothreonine binding sites on their target proteins (41). Sequence analysis of hMex-3B revealed five additional serine/threonine that match 14-3-3 binding sites (data not shown), albeit less stringently than Ser-462. It is, therefore, possible that one of these serine/threonine constitutes a weaker binding site, Ser-462 being the "gatekeeper" residue on which the first interaction with 14-3-3s relies. Alternatively, 14-3-3s may either bring to close proximity two distinct hMex-3B monomers or facilitate the coupling in the same complex of one hMex-3B molecule with another 14-3-3 target that might modulate hMex-3B function, as demonstrated for the kinases Raf-1 and protein kinase Cζ (42).

It is already documented that 14-3-3s mediate regulatory effects on RNA-binding proteins (43–46). Interestingly, the binding of 14-3-3s to the meiotic regulator Mei2p in *Saccharomyces pombe* prevents RNA recognition, a situation reminiscent of what we observed with hMex-3B (47). Also, 14-3-3s bind to the phosphorylated form of the tristetraprolin protein (TTP) and inhibit its ability to trigger the degradation of AU-rich element-containing transcripts (33, 48). However, in the latter case, the TTP-14-3-3 complex binds AU-rich element mRNA, and 14-3-3s is supposed to preclude the directing of both TTP and bound mRNA to the degradative apparatus. Our study suggests a novel mode of regulation with 14-3-3s eliciting cumulative effects on its target, including stabilization of the client protein, interference with the binding on mRNA caused either by a conformational change or a steric hin-

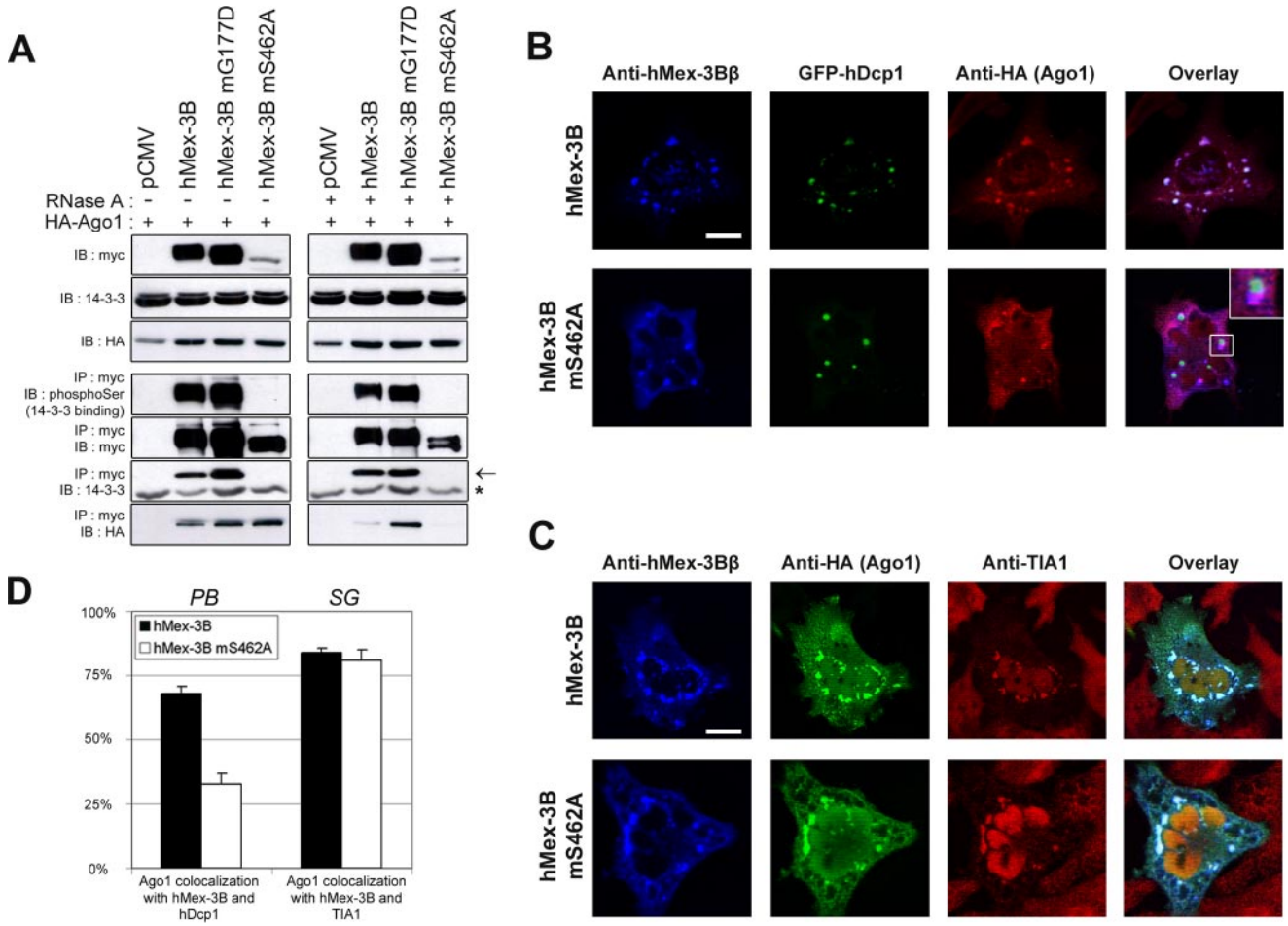

FIGURE 9. **Localization of hMex-3B/Ago1 complexes is regulated through the binding of 14-3-3.** *A*, hMex-3B–Ago1 interaction is dependent on 14-3-3 binding to hMex-3B. BOSC cells were transiently transfected with vectors expressing HA-Ago1 and Myc-tagged wild-type or mutant hMex-3B. Immunoprecipitations (*IP*) were performed using anti-Myc antibody. Samples were loaded on a 11% SDS-polyacrylamide gel, and immunoblot (*IB*) analyses were performed after immunoprecipitation or directly on the lysate with the indicated antibodies. When indicated (+), cell lysates were treated with RNase A (0.2 mg/ml) for 30 min at room temperature. *Arrow*, 14-3-3 proteins. *, IgG light chain. *B* and *D*, colocalization of Ago1 and hMex-3B with PB (*B*) and SG (*C*) markers. Vectors coding hMex-3B and HA-Ago1 were transfected to HeLa cells with (*B*) or without (*C*) cotransfection of hDcp1-GFP. Proteins were stained with anti-hM3Bβ (*blue*) and anti-HA (*B*, *red*; *C*, *green*) antibodies and revealed with AMCA- and Cy5- or Cy2-conjugated secondary antibodies, respectively. hDcp1 protein localization was visualized with GFP fluorescence (*green*) (*B*). TIA1 protein was visualized with anti-TIA1 antibody revealed with a Cy5-conjuged secondary antibody (*C*). Protein localization was determined by confocal microscopy. The *right panel* shows the overlay of AMCA, GFP/Cy2, and Cy5 signal. *Scale bar*, 10 μm. *D*, Ago1 association to PB or SG was quantified in cells expressing either wild-type or mS462A mutant hMex-3B. *Histograms* represent quantification of three independent experiments. *Error bars*, S.D.

drance effect, and finally, differential recruitment to distinct classes of RNA granules.

14-3-3s Are RNA Granules Sorting Modulators—We have previously reported that hMex-3A and hMex-3B are recruited to PBs (14), whereas hMex-3C and hMex-3D are diffusely distributed in the cytoplasm.[5] The present work confirms these results and provides evidence that hMex-3B is also localized in SG and induces the formation of these structures. Similar findings have already been described for a subset of SG-associated molecules whose overexpression results in SG assembly in absence of additional stress, most probably through the aggregation of mRNPs containing these proteins (48–50). Our study further establishes that hMex-3B expression promotes the fusion between SG and PBs. These results are based on confocal microscopy analyses which clearly identified large cytoplasmic foci containing both SG markers, such as TIA1 or eIF4G and PBs markers like hDcp1 and HEDLS. It is unlikely that this phenomenon simply reflects a hMex-3B protein overloading effect as expression of the hMex-3B KH and the S462A mutants did not result in the same phenotype and hMex-3B containing granules are disrupted by cycloheximide treatment. Furthermore, a fusion between these two classes of RNA granules has already been observed upon expression of certain RNA-binding proteins, such as TTP, BRF1, or cytoplasmic polyadenylation element-binding protein (11, 12). In fact, time-lapse video microscopy experiments have unambiguously established that PBs are highly motile structures that transiently interact with SG (11). This dynamic docking process is supposed to facilitate the export of mRNAs destined to be degraded from SG triage centers to the PBs sites of decay. Consistent with these findings, several types of RNA foci, including PBs, SG, and germ granules have been recently described in embryonic blastomeres and in the germline of *C. elegans* (51–53). Interestingly, these granules were also found to be dynamic structures that change compo-

[5] J. Courchet, K. Buchet-Poyau, and M. Billaud, unpublished observation.

sition and interact with each other. Furthermore, Jud *et al.* (53) have provided clear evidence that environmental stresses induce in *C. elegans*-arrested oocytes the formation of large mRNP foci containing Mex-3 and components of both PBs and SG, a finding consistent with our data. It is, thus, possible that hMex-3B itself or in association with other components of SG and PBs stabilizes the interaction between these two compartments and promotes the reconfiguration of mRNP pools leading to the fusion between SG and PBs. Recently, it has been found that the protein involved in type 2 spinocerebellar ataxia, ataxin-2, participates in the assembly of SG and PBs (54). Because the *C. elegans* ortholog of ataxin-2 regulates germline development, an activity requiring MEX-3 (55), it is possible that hMex-3B intersects with the ataxin-2 pathway.

Mutation of Ser-462 disrupts the apparent recruitment of hMex-3B to PBs. Furthermore, expression of Difopein precludes the localization of hMex-3B in PBs but not in SG. These observations raise two possible interpretations, not mutually exclusive; (i) the fixation of 14-3-3 is required for the transport of hMex-3B from SG to PBs; (ii) the hMex-3B:14-3-3 complex stabilizes the labile association between SG and PBs, thus favoring the fusion of these granules. Interestingly, 14-3-3s have the ability to nucleate multicomponent protein complexes, a feature consistent with the idea that proteins may stabilize SG-PBs physical interaction by building up scaffolds that contain SG and PBs subunits (11). This mechanism would favor the delivery of mRNA bound to hMex-3B to the degradation machinery contained in PBs. One can envision that this process is integrated with cellular state and triggered in response to a signal that activates the kinase that phosphorylates Ser-462. The stress-activated protein kinase (mitogen-activated protein kinase-activated protein kinase 2) MK2 phosphorylates TTP on its 14-3-3 binding sites, thus excluding the TTP:14-3-3 complex from SG (48). A similar sensing mechanism may involve the phosphorylation of hMex-3B, a question we are currently addressing.

Ago proteins are components of the RNA-induced silencing complex and are crucial effectors of RNA silencing. Recent studies have revealed that Ago accumulates in SG as well as in PBs (36, 37, 56) and displays dynamic exchange with the cytoplasmic pool, rapid at SG and slower at PBs (37). Furthermore, Ago localization to SG, and not to PBs, requires the presence of microRNAs. We have previously found that hMex-3A and hMex-3B form a complex with Ago1 and Ago2 in a RNA-dependent manner (14). We show here that Ago proteins are retained in SG when the hMex-3B mutant, unable to bind 14-3-3, is expressed. It is, thus, possible that hMex-3B in association with Ago participates to mi-RNA guided translational inhibition in SG, a mechanism regulated by phosphorylation of hMex-3B and the subsequent binding to 14-3-3. Consistent with this idea, several processes linking proteins binding to the 3′UTR of transcripts and the microRNA machinery have been recently described (57).

Taken together, our data sustain the model positing that SG behaves as triage centers that ferry mRNA either to the degradation machinery concentrated in PBs or to the cytoplasm where translation is reinitiated on polysomes (11). They further indicate that the reversible binding of 14-3-3s on RNA-binding proteins contained in the granules may directly impact on mRNA sorting between SG and PBs. Clearly, identification of the mRNAs, which are the physiological targets of hMex-3, will help to gain insight to the underlying mechanisms.

Mex-3 and 14-3-3; a Conserved Mechanism of Action?—During embryonic development of the nematode *C. elegans*, Mex-3 protein transduces information downstream of the PAR polarity proteins, although the mechanistic links remain to be determined (18, 58). Interestingly, PAR-5 belongs to the 14-3-3 family (59), and phosphorylation of the PAR-3 adaptor by the PAR-1 kinase creates a binding site for PAR-5/14-3-3 (60, 61), these molecular interactions contributing to the local establishment of cortical domains in polarized cells. Thus, upon phosphorylation by an upstream kinase, PAR-5/14-3-3 may bind to and regulate Mex-3 function in the nematode and in other species. Similarly, the association between hMex-3B and 14-3-3 might depend on the phosphorylation by a protein kinase involved in cell polarity, an idea deserving to be explored.

Acknowledgments—We are grateful to H. LeHir and T. Renno for advice and critical reading of the manuscript. We thank I. Zanella-Cleon and M. Becchi for technical expertise in mass spectrometry analyses and D. Ressnikoff and Y. Tourneur for support and advice for confocal microscopy analyses. We thank M. Donnini for help in cloning hMex-3D cDNA. We are grateful to B. Seraphin, B. Ducommun, M. Piechaczyk, T. Tuschl, H. Fu, and K. Blackwell for kindly providing reagents.

REFERENCES

1. Sheth, U., and Parker, R. (2003) *Science* **300,** 805–808
2. Teixeira, D., Sheth, U., Valencia-Sanchez, M. A., Brengues, M., and Parker, R. (2005) *RNA* **11,** 371–382
3. Anderson, P., and Kedersha, N. (2006) *J. Cell Biol.* **172,** 803–808
4. Eulalio, A., Behm-Ansmant, I., and Izaurralde, E. (2007) *Nat. Rev. Mol. Cell Biol.* **8,** 9–22
5. Cougot, N., Babajko, S., and Seraphin, B. (2004) *J. Cell Biol.* **165,** 31–40
6. van Dijk, E., Cougot, N., Meyer, S., Babajko, S., Wahle, E., and Seraphin, B. (2002) *EMBO J.* **21,** 6915–6924
7. Ingelfinger, D., Arndt-Jovin, D. J., Luhrmann, R., and Achsel, T. (2002) *RNA* **8,** 1489–1501
8. Durand, S., Cougot, N., Mahuteau-Betzer, F., Nguyen, C. H., Grierson, D. S., Bertrand, E., Tazi, J., and Lejeune, F. (2007) *J. Cell Biol.* **178,** 1145–1160
9. Kedersha, N. L., Gupta, M., Li, W., Miller, I., and Anderson, P. (1999) *J. Cell Biol.* **147,** 1431–1442
10. Bhattacharyya, S. N., Habermacher, R., Martine, U., Closs, E. I., and Filipowicz, W. (2006) *Cell* **125,** 1111–1124
11. Kedersha, N., Stoecklin, G., Ayodele, M., Yacono, P., Lykke-Andersen, J., Fritzler, M. J., Scheuner, D., Kaufman, R. J., Golan, D. E., and Anderson, P. (2005) *J. Cell Biol.* **169,** 871–884
12. Wilczynska, A., Aigueperse, C., Kress, M., Dautry, F., and Weil, D. (2005) *J. Cell Sci.* **118,** 981–992
13. Donnini, M., Lapucci, A., Papucci, L., Witort, E., Jacquier, A., Brewer, G., Nicolin, A., Capaccioli, S., and Schiavone, N. (2004) *J. Biol. Chem.* **279,** 20154–20166
14. Buchet-Poyau, K., Courchet, J., Le Hir, H., Seraphin, B., Scoazec, J. Y., Duret, L., Domon-Dell, C., Freund, J. N., and Billaud, M. (2007) *Nucleic Acids Res.* **35,** 1289–1300
15. Draper, B. W., Mello, C. C., Bowerman, B., Hardin, J., and Priess, J. R. (1996) *Cell* **87,** 205–216
16. Hunter, C. P., and Kenyon, C. (1996) *Cell* **87,** 217–226
17. Ciosk, R., DePalma, M., and Priess, J. R. (2006) *Science* **311,** 851–853
18. Huang, N. N., Mootz, D. E., Walhout, A. J., Vidal, M., and Hunter, C. P.

(2002) *Development* **129,** 747–759
19. Hermeking, H. (2003) *Nat. Rev. Cancer* **3,** 931–943
20. Wilker, E. W., Grant, R. A., Artim, S. C., and Yaffe, M. B. (2005) *J. Biol. Chem.* **280,** 18891–18898
21. Kedersha, N., and Anderson, P. (2007) *Methods Enzymol.* **431,** 61–81
22. Rigaut, G., Shevchenko, A., Rutz, B., Wilm, M., Mann, M., and Seraphin, B. (1999) *Nat. Biotechnol.* **17,** 1030–1032
23. Nony, P., Gaude, H., Rossel, M., Fournier, L., Rouault, J. P., and Billaud, M. (2003) *Oncogene* **22,** 9165–9175
24. Puig, O., Caspary, F., Rigaut, G., Rutz, B., Bouveret, E., Bragado-Nilsson, E., Wilm, M., and Seraphin, B. (2001) *Methods* **24,** 218–229
25. Masters, S. C., Pederson, K. J., Zhang, L., Barbieri, J. T., and Fu, H. (1999) *Biochemistry* **38,** 5216–5221
26. Yaffe, M. B., Rittinger, K., Volinia, S., Caron, P. R., Aitken, A., Leffers, H., Gamblin, S. J., Smerdon, S. J., and Cantley, L. C. (1997) *Cell* **91,** 961–971
27. Hoffmeister, M., Riha, P., Neumuller, O., Danielewski, O., Schultess, J., and Smolenski, A. P. (2008) *J. Biol. Chem.* **283,** 2297–2306
28. Vander Haar, E., Lee, S. I., Bandhakavi, S., Griffin, T. J., and Kim, D. H. (2007) *Nat. Cell Biol.* **9,** 316–323
29. Masters, S. C., and Fu, H. (2001) *J. Biol. Chem.* **276,** 45193–45200
30. Margolis, S. S., Walsh, S., Weiser, D. C., Yoshida, M., Shenolikar, S., and Kornbluth, S. (2003) *EMBO J.* **22,** 5734–5745
31. Chen, H. K., Fernandez-Funez, P., Acevedo, S. F., Lam, Y. C., Kaytor, M. D., Fernandez, M. H., Aitken, A., Skoulakis, E. M., Orr, H. T., Botas, J., and Zoghbi, H. Y. (2003) *Cell* **113,** 457–468
32. Benjamin, D., Schmidlin, M., Min, L., Gross, B., and Moroni, C. (2006) *Mol. Cell. Biol.* **26,** 9497–9507
33. Hitti, E., Iakovleva, T., Brook, M., Deppenmeier, S., Gruber, A. D., Radzioch, D., Clark, A. R., Blackshear, P. J., Kotlyarov, A., and Gaestel, M. (2006) *Mol. Cell. Biol.* **26,** 2399–2407
34. Mackintosh, C. (2004) *Biochem. J.* **381,** 329–342
35. Hu, C. D., and Kerppola, T. K. (2003) *Nat. Biotechnol.* **21,** 539–545
36. Liu, J., Valencia-Sanchez, M. A., Hannon, G. J., and Parker, R. (2005) *Nat. Cell Biol.* **7,** 719–723
37. Leung, A. K., Calabrese, J. M., and Sharp, P. A. (2006) *Proc. Natl. Acad. Sci. U. S. A.* **103,** 18125–18130
38. Tzivion, G., and Avruch, J. (2002) *J. Biol. Chem.* **277,** 3061–3064
39. Muslin, A. J., Tanner, J. W., Allen, P. M., and Shaw, A. S. (1996) *Cell* **84,** 889–897
40. Ganguly, S., Weller, J. L., Ho, A., Chemineau, P., Malpaux, B., and Klein, D. C. (2005) *Proc. Natl. Acad. Sci. U. S. A.* **102,** 1222–1227
41. Yaffe, M. B. (2002) *FEBS Lett.* **513,** 53–57
42. Van Der Hoeven, P. C., Van Der Wal, J. C., Ruurs, P., Van Dijk, M. C., and Van Blitterswijk, J. (2000) *Biochem. J.* **345,** 297–306
43. Schmidlin, M., Lu, M., Leuenberger, S. A., Stoecklin, G., Mallaun, M., Gross, B., Gherzi, R., Hess, D., Hemmings, B. A., and Moroni, C. (2004) *EMBO J.* **23,** 4760–4769
44. Kim, H. H., Abdelmohsen, K., Lal, A., Pullmann, R., Jr., Yang, X., Galban, S., Srikantan, S., Martindale, J. L., Blethrow, J., Shokat, K. M., and Gorospe, M. (2008) *Genes Dev.* **22,** 1804–1815
45. He, C., and Schneider, R. (2006) *EMBO J.* **25,** 3823–3831
46. Gherzi, R., Trabucchi, M., Ponassi, M., Ruggiero, T., Corte, G., Moroni, C., Chen, C. Y., Khabar, K. S., Andersen, J. S., and Briata, P. (2006) *PLoS Biol.* **5,** e5
47. Sato, M., Watanabe, Y., Akiyoshi, Y., and Yamamoto, M. (2002) *Curr. Biol.* **12,** 141–145
48. Stoecklin, G., Stubbs, T., Kedersha, N., Wax, S., Rigby, W. F., Blackwell, T. K., and Anderson, P. (2004) *EMBO J.* **23,** 1313–1324
49. Tourriere, H., Chebli, K., Zekri, L., Courselaud, B., Blanchard, J. M., Bertrand, E., and Tazi, J. (2003) *J. Cell Biol.* **160,** 823–831
50. Gilks, N., Kedersha, N., Ayodele, M., Shen, L., Stoecklin, G., Dember, L. M., and Anderson, P. (2004) *Mol. Biol. Cell* **15,** 5383–5398
51. Gallo, C. M., Munro, E., Rasoloson, D., Merritt, C., and Seydoux, G. (2008) *Dev. Biol.*, in press
52. Noble, S. L., Allen, B. L., Goh, L. K., Nordick, K., and Evans, T. C. (2008) *J. Cell Biol.* **182,** 559–572
53. Jud, M. C., Czerwinski, M. J., Wood, M. P., Young, R. A., Gallo, C. M., Bickel, J. S., Petty, E. L., Mason, J. M., Little, B. A., Padilla, P. A., and Schisa, J. A. (2008) *Dev. Biol.* **318,** 38–51
54. Nonhoff, U., Ralser, M., Welzel, F., Piccini, I., Balzereit, D., Yaspo, M. L., Lehrach, H., and Krobitsch, S. (2007) *Mol. Biol. Cell* **18,** 1385–1396
55. Ciosk, R., DePalma, M., and Priess, J. R. (2004) *Development* **131,** 4831–4841
56. Pillai, R. S., Bhattacharyya, S. N., Artus, C. G., Zoller, T., Cougot, N., Basyuk, E., Bertrand, E., and Filipowicz, W. (2005) *Science* **309,** 1573–1576
57. Jing, Q., Huang, S., Guth, S., Zarubin, T., Motoyama, A., Chen, J., Di Padova, F., Lin, S. C., Gram, H., and Han, J. (2005) *Cell* **120,** 623–634
58. Bowerman, B., Ingram, M. K., and Hunter, C. P. (1997) *Development* **124,** 3815–3826
59. Morton, D. G., Shakes, D. C., Nugent, S., Dichoso, D., Wang, W., Golden, A., and Kemphues, K. J. (2002) *Dev. Biol.* **241,** 47–58
60. Benton, R., Palacios, I. M., and St. Johnston, D. (2002) *Dev. Cell* **3,** 659–671
61. Benton, R., and St. Johnston, D. (2003) *Cell* **115,** 691–704